
Reliable one-bit quantization of bandlimited graph data via single-shot noise shaping

Johannes Maly ^{*1,2} Anna Veselovska ^{*3,2}

Abstract

Graph data are ubiquitous in natural sciences and machine learning. In this paper, we consider the problem of quantizing graph structured, bandlimited data to few bits per entry while preserving its information under low-pass filtering. We propose an efficient single-shot noise shaping method that achieves state-of-the-art performance and comes with rigorous error bounds. In contrast to existing methods it allows reliable quantization to arbitrary bit-levels including the extreme case of using a single bit per data coefficient.

1. Introduction

In various machine learning applications, the data that have to be processed exhibit a graph structure such as in social networks, web information analysis, and sensor networks (Ortega et al., 2018). To reduce data processing costs, research in graph signal processing (GSP) aims to extend well-developed tools from signal processing to graph data by accounting for underlying connectivity (Shuman et al., 2013; Sandryhaila & Moura, 2014). This is possible since graph data often has a favorable spectral structure under application of the Graph Fourier Transform (Dong et al., 2016; Shuman et al., 2016). An interesting question in this context is whether one can leverage the spectral structure to minimize the error induced by quantizing the data representation to few bits per scalar.

The interplay between quantization and GSP has been considered from different angles in the past years. Chamon & Ribeiro (2017) study the effect of finite-precision arithmetics on low-pass graph filters. Nobre & Frossard (2019) propose an optimized quantization scheme for reducing the message transmission between nodes when applying polynomial filtering to graph data in a distributed way. In a similar distributed setting, Ben Saad et al. (2022) examine

the noise induced by dithered quantizers when applying different types of filtering to graph data.

Various works have investigated how graph data can be reconstructed from few quantized samples. Di Lorenzo et al. (2018); Kim & Ortega (2019) empirically examine the algorithmic reconstruction of graph data from noisy samples that have been quantized by a memoryless scalar quantizer. Li et al. (2021; 2022) consider optimal task-based quantization by fixing a bandlimited signal on a graph and optimizing the quantization scheme. Kim (2022) proposes a greedy algorithm to select an optimal sampling set on which the discrepancy between a bandlimited ground-truth and its naively quantized counterpart is minimized.

Our work is closely related to the works of Krahmer et al. (2023; 2026) and Reingruber & Matz (2025) which aim at robust quantization without subsampling. Krahmer et al. (2023; 2026) use $\Sigma\Delta$ -quantization to quantize bandlimited graph data to few bits per entry. Reingruber & Matz (2025) use local graph Fourier frames to extract a quantized representation. In contrast to the works of Krahmer et al. (2023; 2026) and us, Reingruber & Matz (2025) use overcomplete frames, which leads to a higher-dimensional quantized representation.

Finally, we remark that graph data may exhibit structural properties beyond low-bandwidth behavior (Tanaka & Elgar, 2020). In addition, efficient quantization of graph signals plays an important role in enabling scalable training of *Graph Neural Networks (GNNs)* (Courbariaux et al., 2015; Tailor et al., 2021).

1.1. Contribution

In this paper, we propose a novel single-shot noise shaping method for quantizing graph data. It draws inspiration from a recent result of Maly & Saab (2023) on neural network quantization. Similar to the approach of Krahmer et al. (2023; 2026), our method translates an N -dimensional graph structured signal into an N -dimensional quantized representation. In contrast to this existing method — which is computationally favorable, but restricted to using $\log \log(N)$ bits per entry — *our approach allows flexible tuning of the bit-level, including the extreme case of using a*

^{*}Equal contribution ¹Department of Mathematics, Ludwig-Maximilians-Universität, Munich, Germany ²Munich Center for Machine Learning, Munich, Germany ³Department of Mathematics and Munich Data Science Institute, Technical University of Munich, Munich, Germany.

single bit per data coefficient. Furthermore, it comes with slightly improved theoretical worst-case guarantees and a strongly simplified proof strategy.

Roadmap. Section 2 introduces notation and basic concepts from graph signal processing. In Section 3, we present the proposed single-shot noise shaping (SSNS) quantization method for bandlimited graph data and state our theoretical guarantees, explaining the relation to the work of Maly & Saab (2023) and comparing our guarantees with existing iterative noise-shaping approaches. Section 4 presents numerical experiments on several graph topologies, validating the theoretical scaling and demonstrating practical performance.

1.2. Notation

In the following, we will abbreviate index sets as $[N] = \{1, \dots, N\}$. We will use bold lowercase and uppercase letters to distinguish vectors and matrices from scalars. The Euclidean and the max-norm of a vector $\mathbf{z} \in \mathbb{R}^N$ are denoted by $\|\mathbf{z}\|_2$ and $\|\mathbf{z}\|_\infty$, respectively. The ℓ_2 -operator norm of a matrix $\mathbf{X} \in \mathbb{R}^{n_1 \times n_2}$ is denoted by $\|\mathbf{X}\|$. The $(\ell_2 \rightarrow \ell_\infty)$ -operator norm of \mathbf{X} is denoted by $\|\mathbf{X}\|_{2,\infty}$. Note that $\|\mathbf{X}\|_{2,\infty}$ corresponds to the maximum ℓ_2 -norm of the rows of \mathbf{X} . When applied to a matrix $\mathbf{X}^{n \times n}$, the operator diag extracts its diagonal $\mathbf{x} \in \mathbb{R}^n$; when applied to a vector $\mathbf{x} \in \mathbb{R}^n$, diag returns the corresponding diagonal matrix $\mathbf{X} \in \mathbb{R}^{n \times n}$. We abbreviate $a \leq Cb$, for an absolute constant, by $a \lesssim b$ and write $a \simeq b$ if $a \lesssim b$ and $b \lesssim a$.

2. Preliminaries on graph data

We consider data that lies on an undirected graph $\mathcal{G} = (\mathcal{V}, \mathcal{E}, \mathbf{W})$, where \mathcal{V} is a set of N vertices, \mathcal{E} is a set of edges, and $\mathbf{W} \in \mathbb{R}^{N \times N}$ is a weighted adjacency matrix. Let $d_m := \sum_{n=1}^N W_{mn}$ be the degree of the m th vertex. The normalized Laplacian \mathcal{L} of \mathcal{G} is defined as $\mathcal{L} = \mathbf{D}^{-1/2}(\mathbf{D} - \mathbf{W})\mathbf{D}^{-1/2}$, where $\mathbf{D} = \text{diag}\{(d_1, d_2, \dots, d_N)^T\}$ is the degree matrix. In our setting, \mathcal{L} is symmetric, positive semi-definite and thus has an orthogonal eigenbasis $\mathbf{X} = [\mathbf{x}_1, \mathbf{x}_2, \dots, \mathbf{x}_N]$, where the eigenvectors $\mathbf{x}_1, \dots, \mathbf{x}_N$ have corresponding non-negative eigenvalues $0 \leq \lambda_1 \leq \dots \leq \lambda_N$.

Data on the graph can be represented by a function $f: \mathcal{V} \rightarrow \mathbb{R}$ defined on vertices of the graph. Note that any f is equivalent to a vector $\mathbf{f} \in \mathbb{R}^N$, where the n th component of \mathbf{f} represents the function value at the n -th vertex in \mathcal{V} . The eigenvectors and eigenvalues of the Laplacian \mathcal{L} provide a spectral interpretation of the graph. Indeed, the eigenvalues $\{\lambda_1, \lambda_2, \dots, \lambda_N\}$ can be interpreted as graph frequencies, while the eigenvectors demonstrate increasing oscillatory behavior as the magnitude of the graph frequencies increases (Shuman et al., 2016). Based on this interpreta-

tion, the *Graph Fourier Transform (GFT)* of \mathbf{f} is defined as $\widehat{\mathbf{f}} = \mathbf{X}^T \mathbf{f} \in \mathbb{R}^N$ with entries $\widehat{\mathbf{f}}(\lambda_i) = \langle \mathbf{f}, \mathbf{x}_i \rangle$.

In applications, graph data often exhibit intrinsic structure that can be leveraged for efficient data processing, e.g., dominance of low frequencies in the spectral domain (Dong et al., 2016). Graph data \mathbf{f} are called *bandlimited* if there exists $r \in [N]$ such that the support of the GFT of \mathbf{f} is contained in the frequencies $\{\lambda_1, \dots, \lambda_r\}$ (Pesenson, 2009; Shuman et al., 2016).

Let us denote by $\mathbf{X}_r = [\mathbf{x}_1, \dots, \mathbf{x}_r] \in \mathbb{R}^{N \times r}$ the matrix \mathbf{X} restricted to the first r columns. Then every r -bandlimited function \mathbf{f} can be written as $\mathbf{f} = \mathbf{X}_r \boldsymbol{\alpha}$, for some $\boldsymbol{\alpha} \in \mathbb{R}^r$. By re-normalizing our data, we can always assume that $\|\mathbf{f}\|_\infty = 1$. The graph's geometry and properties of its bandlimited function subspaces can be quantified by the *graph incoherence* (Shuman et al., 2016).

Definition 2.1. (Shuman et al., 2016) For the r -dimensional subspace of graph functions spanned by $\mathbf{X}_r = [\mathbf{x}_1, \dots, \mathbf{x}_r] \in \mathbb{R}^{N \times r}$, let $P_{\mathbf{X}_r} = \mathbf{X}_r \mathbf{X}_r^T$ be the orthogonal projection onto \mathbf{X}_r . The *incoherence* of the graph subspace \mathbf{X}_r is defined as

$$\mu(\mathbf{X}_r) = \frac{N}{r} \max_{1 \leq i \leq N} \|P_{\mathbf{X}_r} \mathbf{e}_i\|_2^2. \quad (2.1)$$

It has been shown for various types of random graphs that μ is small with high probability if the respective graph is sufficiently large (Dekel et al., 2011; Brooks & Lindenstrauss, 2013). This indicates that the graph Laplacian eigenvectors are well-spread in general.

3. Quantizing graph data

We are interested in quantizing bandlimited graph data. Given an r -bandlimited graph function $\mathbf{f} \in \mathbb{R}^N$, we aim to construct a quantized representation $\mathbf{q} \in \mathcal{A}^N$ that uses fewer bits per entry, but preserves the important information encoded in \mathbf{f} . Motivated by imaging applications (Floyd, 1976; Fornasier & Hütter, 2016; Huang et al., 2021; Krahmer & Veselovska, 2023; 2025; Lyu & Wang, 2023; Ehler et al., 2021), the resulting quantization error \mathcal{QE} can be quantified by the ℓ_2 -distance between \mathbf{f} and \mathbf{q} under the action of a low-pass graph filter $\mathbf{L} := [\ell_1, \dots, \ell_N] \in \mathbb{R}^{N \times N}$:

$$\mathcal{QE}_{\mathbf{L}}(\mathbf{f}, \mathbf{q}) = \|\mathbf{L}(\mathbf{f} - \mathbf{q})\|_2.$$

We will focus here on the brick-wall filter $\mathbf{L}_r = \mathbf{X}_r \mathbf{X}_r^T$, for which $\mathbf{L}_r \mathbf{f} = \mathbf{f}$, and call $\mathbf{f}_q = \mathbf{L}_r \mathbf{q}$ a quantized representative of \mathbf{f} . For $K \geq 1$, we define *midrise* alphabets having $2K$ elements, as sets of the form

$$\mathcal{A} = \{\pm(k - 1/2)\delta : 1 \leq k \leq K, k \in \mathbb{Z}\}, \quad (3.1)$$

where $\frac{\delta}{2} > 0$ denotes the quantizer resolution on the range $[-K\delta, K\delta]$ of \mathcal{A} . The simplest example is the 1-bit alphabet

Algorithm 1 Vector preprocessing (Maly & Saab, 2023)

Input: $\mathbf{X} \in \mathbb{R}^{r \times N}$ ($r < N$), $\mathbf{z}_0 \in \mathbb{R}^N$, and $c \geq \|\mathbf{z}_0\|_\infty$

Initialize $k = 0$ and

$$J_0 = \{i \in [N] : \text{the } i\text{-th column of } \mathbf{X} \text{ is zero}\}$$

Define $\mathbf{b} \in \mathbb{R}^N$ via $\mathbf{b}_{J_0^c} = \mathbf{0}$ and $b_i = c - (z_0)_i$, for $i \in J_0$, such that $\mathbf{b} \in \ker(\mathbf{X})$ and $|(z_0)_i + b_i| = c$ for $i \in J_0$. Replace \mathbf{z}_0 with $\mathbf{z}_0 + \mathbf{b}$.

repeat

 Compute $\mathbf{b} \in \ker_{J_k}(\mathbf{X})$, $\mathbf{b} \neq \mathbf{0}$

 Compute $\alpha \in \mathbb{R}$ with $\|\mathbf{z}_k + \alpha \mathbf{b}\|_\infty = c$

$$\mathbf{z}_{k+1} \leftarrow \mathbf{z}_k + \alpha \mathbf{b} \in \mathbb{R}^N$$

$$J_{k+1} \leftarrow J_k \cup \{i \in [N] : |(\mathbf{z}_{k+1})_i| = c\}$$

$$k \leftarrow k + 1$$

until $\|\mathbf{z}_k\|_\infty - c\mathbf{1}\|_0 \leq r$

$$k_{\text{final}} = k$$

Output: $\mathbf{z}_{k_{\text{final}}}$ for which $\mathbf{X}\mathbf{z}_{k_{\text{final}}} = \mathbf{X}\mathbf{z}_0$, $\|\mathbf{z}_{k_{\text{final}}}\|_\infty = c$, and $\|\mathbf{z}_{k_{\text{final}}}\|_\infty - c\mathbf{1}\|_0 \leq r$

$\{-1, 1\}$ with (full resolution) range $[-2, 2]$ and quantizer resolution 1.

The *memoryless scalar quantizer* (MSQ) associated with alphabet \mathcal{A} is given by $Q : \mathbb{R} \rightarrow \mathcal{A}$ defined as

$$Q(z) := \arg \min_{p \in \mathcal{A}} |z - p|. \quad (3.2)$$

For $\mathcal{A} = \{-1, 1\}$ the MSQ Q is given by the two-valued sign-function

$$\text{sign}(x) = \begin{cases} 1 & x \geq 0 \\ -1 & x < 0. \end{cases}$$

When applied to vectors, the MSQ Q acts entry-wise. We will call Q a B -bit quantizer if $|\mathcal{A}| = 2^B$. For such a quantizer with target range $[-c, c]$, $c > 0$, the quantizer resolution of the midrise alphabet in (3.1) satisfies $\delta \simeq c2^{-B}$.

3.1. Single-shot noise-shaping (SSNS)

To quantize band-limited graph data \mathbf{f} , we will draw inspiration from recent work on neural network quantization (Maly & Saab, 2023). The authors propose to combine a simple neuron preprocessing algorithm with plain application of MSQ to quantize neurons in feedforward networks while preserving the input-output relation. It turns out that a similar strategy can be used for reliable quantization of bandlimited graph data. Compared to the iterative noise-shaping quantizer of Krahmer et al. (2023; 2026) this approach can be interpreted as a single-shot noise-shaping quantizer, which is also reflected in the name of our method.

We recall the preprocessing algorithm of Maly & Saab (2023) tailored to the graph setting in Algorithm 1. The

main goal of this preprocessing step is to obtain an alternative representation of \mathbf{f} that preserves its low-frequency information while simultaneously minimizing the quantization error when followed by MSQ. Note that in Algorithm 1 we denote the kernel of $\mathbf{A} \in \mathbb{R}^{n_1 \times n_2}$ restricted to $J \subset [n_2]$ by

$$\ker_J(\mathbf{A}) := \{\mathbf{b} \in \ker(\mathbf{A}) : b_i = 0 \text{ if } i \in J\} \quad (3.3)$$

and that $\ker_{J_k}(\mathbf{X}_k) \neq \{\mathbf{0}\}$ as long as $\|\mathbf{z}_k\|_\infty - c\mathbf{1}\|_0 > r$.

To compute a quantized representation \mathbf{q} of \mathbf{f} , we first apply Algorithm 1 to $\mathbf{X} = \mathbf{X}_r^T \in \mathbb{R}^{r \times N}$ with $\mathbf{z}_0 = \mathbf{f}$, and $c = \|\mathbf{f}\|_\infty = 1$. This yields a new representation $\hat{\mathbf{f}} \in \mathbb{R}^N$ of \mathbf{f} for which $\mathbf{X}_r^T \hat{\mathbf{f}} = \mathbf{X}_r^T \mathbf{f}$, $\|\hat{\mathbf{f}}\|_\infty = 1$, and

$$|\{i \in [N] : |\hat{f}_i| \neq 1\}| \leq r. \quad (3.4)$$

In plain words: After preprocessing, all but at most r entries of $\hat{\mathbf{f}}$ lie exactly on the boundary of the unit ℓ_∞ -ball and therefore attain the extreme values ± 1 . This property is crucial: when applying a midrise quantizer with an alphabet including ± 1 , at most r unsaturated entries can contribute nonzero quantization error, while the remaining entries are already elements of the quantization alphabet. Figure 1 illustrates in \mathbb{R}^3 how Algorithm 1 proceeds.

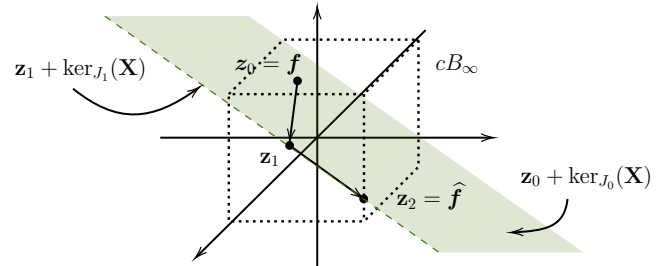


Figure 1. Illustration of Algorithm 1 in \mathbb{R}^3 . The algorithm walks in a kernel direction (green plane) until it hits the boundary of the scaled ℓ_∞ ball cB_∞ such that at least one entry of \mathbf{z}_k is set to $\pm c$. After reducing the feasible kernel directions (dashed green line), the algorithm repeats the procedure until at most r entries of \mathbf{z}_k are not equal to $\pm c$.

Following the preprocessing step, we apply a B -bit quantizer with midrise alphabet $\mathcal{A}_B = \{-1, -1 + \frac{2}{2^B-1}, \dots, 1 - \frac{2}{2^B-1}, 1\}$, i.e., $K = 2^{B-1}$ and $\delta = 4 \cdot 2^{-B}$ to $\hat{\mathbf{f}}$, which yields the quantized representation $\mathbf{q} = Q(\hat{\mathbf{f}})$. The quantization method is summarized in Algorithm 2.

Due to (3.4) and the choice of \mathcal{A} , at most r of the entries of $\hat{\mathbf{f}}$ will contribute to the quantization error $\mathcal{QE}_{L_r}(\mathbf{f}, \mathbf{q})$ in this procedure. We can now bound $\mathcal{QE}_{L_r}(\mathbf{f}, \mathbf{q})$.

Theorem 3.1. *There exists an absolute constant $C > 0$ such that the following holds. Let $\mathcal{G} = (\mathcal{V}, \mathcal{E}, \mathbf{W})$ be an undirected graph. Then, for any r -bandlimited $\mathbf{f} \in \mathbb{R}^N$*

with $\|\mathbf{f}\|_\infty = 1$, we have that \mathbf{q} computed via Algorithm 2 satisfies

$$\frac{\mathcal{QE}_{\mathbf{L}_r}(\mathbf{f}, \mathbf{q})}{\|\mathbf{f}\|_2} \leq C \cdot 2^{-B} \cdot \mu(\mathbf{X}_r) \cdot \frac{r}{\sqrt{N}},$$

where $\mathbf{L}_r = \mathbf{X}_r \mathbf{X}_r^T$ is the brick-wall filter of bandwidth r , i.e., $\mathbf{X}_r \in \mathbb{R}^{N \times r}$ contains the eigenvectors of the normalized Laplacian \mathcal{L} corresponding to the r -smallest eigenvalues of \mathcal{L} .¹

Algorithm 2 B -bit single-shot noise shaping (SSNS)

Input: Graph Laplacian $\mathcal{L} \in \mathbb{R}^{N \times N}$, graph data $\mathbf{f} \in \mathbb{R}^N$ normalized to $\|\mathbf{f}\|_\infty = 1$, bit-level B , target bandwidth $r \in [N]$

- **Preparation:** Compute $\mathbf{X}_r \in \mathbb{R}^{N \times r}$ by eigendecomposition of \mathcal{L}
- **Preprocessing:** Apply Algorithm 1 with $\mathbf{X} = \mathbf{X}_r^T \in \mathbb{R}^{r \times N}$, $\mathbf{z}_0 = \mathbf{f}$, and $c = \|\mathbf{f}\|_\infty = 1$ to obtain the alternative representation $\hat{\mathbf{f}}$ of \mathbf{f} .
- **Quantization:** Apply MSQ Q with B -bit alphabet \mathcal{A}_B ($K = 2^{B-1}$ and $\delta = 4 \cdot 2^{-B}$) to obtain $\mathbf{q} = Q(\hat{\mathbf{f}})$

Output: B -bit approximation \mathbf{q} of \mathbf{f}

In the proof of Theorem 3.1, we will use the following insight from Maly & Saab (2023).

Theorem 3.2 (Maly & Saab (2023, Theorem 2.2)). *Let $N_0 > m$ be natural numbers, let $\mathbf{w} \in \mathbb{R}^{N_0}$, and let $\mathbf{X} \in \mathbb{R}^{N_0 \times m}$. Define the data complexity parameter*

$$\Gamma(\mathbf{X}) = \sup_{\substack{T \subset [N_0] \\ |T|=m}} \|\mathbf{X}^T|_T\|$$

where $\mathbf{X}^T|_T \in \mathbb{R}^{m \times m}$ denotes the submatrix of \mathbf{X}^T with columns indexed by T . For Q as defined in Algorithm 2 and $\mathbf{q} = Q(\hat{\mathbf{w}})$ with $\hat{\mathbf{w}}$ being the output of Algorithm 1 with inputs \mathbf{X}^T , \mathbf{w} , and $\|\mathbf{w}\|_\infty$, we have that

$$\|\mathbf{X}^T \mathbf{w} - \mathbf{X}^T \mathbf{q}\|_2 \leq C \cdot 2^{-B} \cdot \Gamma(\mathbf{X}) \cdot \sqrt{m} \cdot \|\mathbf{w}\|_\infty.$$

Proof of Theorem 3.1. First note that

$$\mathcal{QE}_{\mathbf{L}_r}(\mathbf{f}, \mathbf{q}) = \|\mathbf{X}_r \mathbf{X}_r^T(\mathbf{f} - \mathbf{q})\|_2 = \|\mathbf{X}_r^T(\mathbf{f} - \mathbf{q})\|_2,$$

where we used that the columns of \mathbf{X}_r are orthogonal. Applying Theorem 3.2 to the right-hand side with $N_0 = N$, $m = r$, $\mathbf{w} = \mathbf{f}$ with $\|\mathbf{f}\|_\infty = 1$, and $\mathbf{X} = \mathbf{X}_r$ then yields

$$\mathcal{QE}_{\mathbf{L}_r}(\mathbf{f}, \mathbf{q}) \leq C \cdot 2^{-B} \cdot \Gamma(\mathbf{X}_r) \cdot \sqrt{r}.$$

¹In the case that the smallest r eigenvalues are not unique, we fix any non-decreasing order and choose the first r .

Since \mathbf{X}_r has orthogonal columns, $\Gamma(\mathbf{X}_r) \leq \|\mathbf{X}_r\| = 1$. Furthermore, since \mathbf{f} is r -bandlimited, we obtain

$$\begin{aligned} 1 &= \|\mathbf{f}\|_\infty = \|\mathbf{X}_r \mathbf{a}\|_\infty \leq \|\mathbf{X}_r\|_{2,\infty} \|\mathbf{a}\|_2 \\ &\leq \mu(\mathbf{X}_r) \sqrt{\frac{r}{N}} \cdot \|\mathbf{a}\|_2, \end{aligned}$$

for some $\mathbf{a} \in \mathbb{R}^r$ with $\|\mathbf{a}\|_2 = \|\mathbf{f}\|_2$, where we used that $\mu(\mathbf{X}_r) \geq \frac{N}{r} \|\mathbf{X}_r\|_{2,\infty}$ by definition. Since this implies that $\|\mathbf{f}\|_2 \geq \mu(\mathbf{X}_r)^{-1} \sqrt{\frac{N}{r}}$, we obtain our claimed bound

$$\frac{\mathcal{QE}_{\mathbf{L}_r}(\mathbf{f}, \mathbf{q})}{\|\mathbf{f}\|_2} \leq \frac{C \cdot 2^{-B} \cdot \sqrt{r}}{\|\mathbf{f}\|_2} \leq C 2^{-B} \mu(\mathbf{X}_r) \frac{r}{\sqrt{N}}.$$

□

3.2. Comparison with iterative noise-shaping methods

Let us compare Theorem 3.1 with existing results of Krahmer et al. (2023; 2026) on quantizing bandlimited graph data via iterative noise shaping. Their algorithm iteratively samples with replacement M graph vertices at random, and quantizes the corresponding entry of \mathbf{f} to the alphabet \mathcal{A} depending on the accumulated quantization error so far. If single vertices have been selected and quantized multiple times, e.g., for $M > N$, these results are accumulated to derive a quantized representation $\mathbf{q} \in \tilde{\mathcal{A}}^N$ of \mathbf{f} . Here $\tilde{\mathcal{A}}$ is an augmented alphabet with $|\tilde{\mathcal{A}}| \lesssim |\mathcal{A}| \log(N)$ if $M = \mathcal{O}(N \log(N))$.

In the extreme case of using a one-bit quantizer with $\mathcal{A} = \{-1, 1\}$ and setting $M = N \log(N)$, Theorem IV.1 in Krahmer et al. (2023) shows that

$$\frac{\mathcal{QE}_{\mathbf{L}_r}(\mathbf{f}, \mathbf{q})}{\|\mathbf{f}\|_2} \lesssim \mu(\mathbf{X}_r) \frac{r \log(r)}{\sqrt{N \log(N)}}. \quad (3.5)$$

It is important to note that this result requires a total bit budget of $N \log(\log(N))$ bits (Krahmer et al., 2023; 2026).

If we use the same total bit budget with our method, this corresponds to $B = \log(\log(N))$ since we are quantizing exactly N entries of \mathbf{f} . In this case, the bound in Theorem 3.1 becomes

$$\frac{\mathcal{QE}_{\mathbf{L}_r}(\mathbf{f}, \mathbf{q})}{\|\mathbf{f}\|_2} \lesssim \mu(\mathbf{X}_r) \frac{r}{\sqrt{N \log(N)}}. \quad (3.6)$$

Apparently, the theoretical error bound of our method surpasses the one of Krahmer et al. (2023; 2026). This is particularly remarkable as our approach is based on single-shot noise shaping before quantization while the work of Krahmer et al. (2023; 2026) adaptively shapes the noise during quantization. What is more, the comparison shows that the method of Krahmer et al. (2023; 2026) does not allow a final quantization level of only one bit per entry as soon as \mathcal{A} is augmented in the final representation.

Our experiments on a ring graph in Section 4 suggest that the worst-case bound in Theorem 3.1 is tight. At the same time, they show that such worst-case guarantees might be too conservative in general since the empirical performance of the investigated methods considerably surpasses the predicted bounds on several graphs.

4. Numerical Experiments

We present numerical experiments to evaluate the performance of the proposed Single-Shot Noise Shaping (SSNS) method and to compare it with existing quantization schemes. The experiments examine the effect of graph topology, bandwidth, and bit budget on reconstruction accuracy, verify our theory, and demonstrate its practical behavior on a 3D shape halftoning task.

While Algorithm 1 is well suited to convey the concept of our noise shaping approach, it requires $\mathcal{O}(r^3 N)$ operations in the worst case. Meyer (2024) developed a more efficient implementation of Algorithm 1 reducing this to $\mathcal{O}(r^2 N)$ operations. In our experiments, we will exclusively use the superior version of Meyer (2024), which is summarized in Algorithm 3 in the supplementary material, and refer to it as *Single Shot Noise Shaping (SSNS)*.

Experiment 1: Quantization Error vs. Bandwidth Across Graph Topologies. We begin by evaluating the performance of SSNS on several standard graph topologies, including *grid*, *bunny*, *ring*, *Swiss-roll*, *sensor* and *Minnesota* graphs. For each graph, we consider low-pass graph data $\mathbf{f} = \mathbf{X}, \boldsymbol{\alpha}$ of varying bandwidths $r \in [15, 155]$, generated with Gaussian $\boldsymbol{\alpha} \in \mathbb{R}^r$, which is normalized to have $\|\mathbf{f}\|_\infty = 1$.

We perform experiments with multiple bit budgets, $B \in \{1, 2, 4\}$, using 20 independent realizations of the data for each bandwidth. SSNS is applied to each realization, and the quantization error is measured by the *Relative Error* in ℓ_2 -norm after applying a brick-wall filter or bandwidth r , i.e.,

$$\text{Relative Error} = \frac{\mathcal{Q}\mathcal{E}_{\mathbf{L}_r}(\mathbf{f}, \mathbf{q})}{\|\mathbf{f}\|_2} = \frac{\|\mathbf{L}_r(\mathbf{f} - \mathbf{q})\|_2}{\|\mathbf{f}\|_2} \quad (4.1)$$

Figure 2 shows the Relative Error of SSNS as a function of the bandwidth for each graph, on a semi-logarithmic scale and averaged over the random realizations. Each curve corresponds to a different bit budget ($B = 1, 2, 4$). We observe the following.

- As the number of bits increases, the average relative error decreases consistently across all graphs, confirming the expected trade-off between bit budget and quantization error. We further investigate this in Experiment 2.
- Overall, lower bandwidth induces lower quantization errors, due to low-bandwidth data being concentrated

in fewer Fourier modes. However, we note that on certain graphs such as *bunny* or *sensor* this trend is reversed for very small bandwidths. So far, we could not find a satisfactory explanation of this peculiar behavior; it is also not reflected in our worst-case error bound, cf. Experiment 3. However, we suspect that this is related to the structure of the first eigenvectors, which are more dominant for low-bandwidth signals.

Figure 3 compares the quantized representations $\mathbf{f}_q = \mathbf{L}_r \mathbf{q}$ of an exemplary data sample on the *bunny* graph with their unquantized counterpart. The figure visualizes how well low-bandwidth data on graphs can be preserved by coarsely quantized samples. Furthermore, Figure 3 (f)–(h) suggests that, under our single-shot noise shaping approach, the quantization error accumulates at “high-curvature” regions of the graph. It would be desirable to understand this effect in future work.

Experiment 2: Empirical and Theoretical Bit-Depth Scaling. In this experiment, we investigate the effect of quantization bit-depth on the reconstruction accuracy of bandlimited graph signals under the SSNS method, and compare its empirical performance with our theoretical error bounds. We consider the same graph topologies as in Experiment 1. For each graph, we generate bandlimited graph signals supported on the first $r = 200$ graph Fourier modes, and generate 50 independent signal realizations. We measure the relative squared reconstruction error (4.1) and report the average error over all realizations for each bit-depth.

The theoretical analysis predicts that the reconstruction error scales as $\mathcal{O}(2^{-B})$ if r and N are fixed. In Figure 5, we display this bound (up to a constant factor) together with the average relative error. We see that for small bit rates the actual average error is considerably smaller than expected. Note that this does not contradict our error bounds which are based on worst-case estimates.

Experiment 3: SSNS vs. SSS-R and Worst-Case Error Guarantees. Finally, we compare the performance of SSNS to our theoretical worst-case guarantees in Theorem 3.1 and to the *Step-by-Step-Serving with Replacement* (SSS-R) method of Krahmer et al. (2023; 2026) under a fixed quantization budget of $\log \log N$ bits required by the SSS-R method, cf. Section 3.2. Figure 4 reports the Relative Error (on logarithmic scale) as a function of r for several representative graph topologies, including *grid*, *ring*, and *Swiss-roll* graphs. For each bandwidth value, the reported error is obtained by averaging over multiple random realizations.

We compare our proposed SSNS method with the baseline SSS-R scheme. Across all graph models, SSNS consistently attains lower or comparable average relative error for small to moderate bandwidths. As the bandwidth increases, the

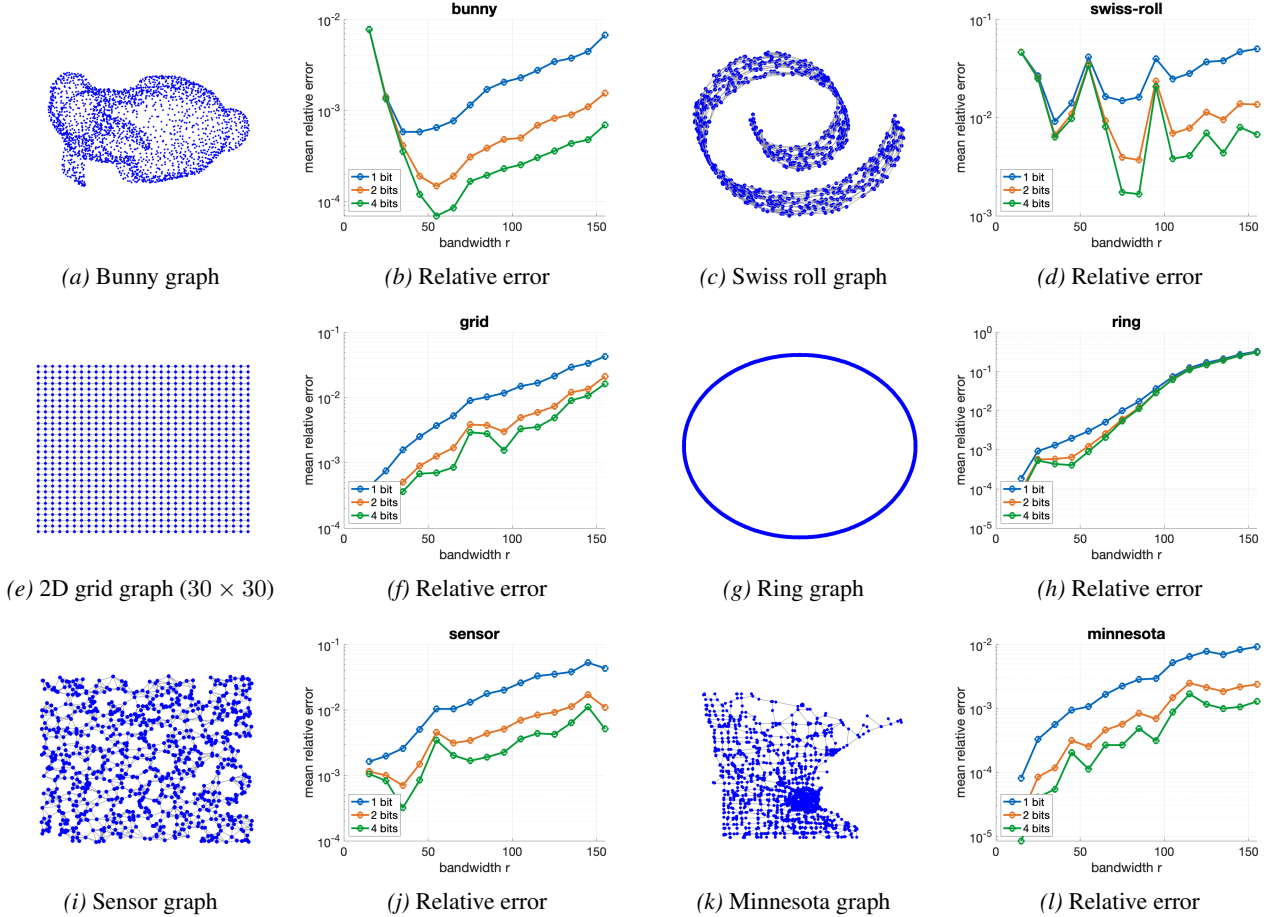


Figure 2. Performance of the proposed SSNS quantization algorithm on different graph structures. For each graph (left), the corresponding semilog plot of the relative reconstruction error (right) is shown for different quantization bit budgets $B = 1, 2, 4$.

error of both methods grows, reflecting the increased incoherence of the graph Fourier basis associated with larger neighborhoods. For larger bandwidths, SSS-R shows more stability and achieves lower error. Let us mention that SSS-R only requires $\mathcal{O}(rN \log(N))$ operations, which makes it more efficient for higher bandwidths. However, SSS-R is not available for 1-bit quantization and always requires $N \log(N)$ -bits on average.

The dashed curves correspond to the theoretical upper bound in (3.6). In particular, we see that our theoretical bound is tight for the ring graph. For the remaining graphs, it is overly pessimistic due to its worst-case nature, but accurately captures the overall growth trend with respect to r and provides theoretical justification for the observed degradation in performance at larger bandwidths. Importantly, SSNS remains well below the theoretical bound across all considered graphs, confirming its robustness to quantization effects.

Experiment 4: Graph-Signal Halftoning on 3D Meshes.
Finally, we evaluate the proposed SSNS algorithm for

halftoning of graph signals on 3D shapes and compare it with Sigma-Delta-Weight (SDW) in (Krahmer et al., 2023) and *memoryless scalar quantization* (MSQ); see also related work on 3D halftoning in (Gooran & Abedini, 2020, 2022; Mao et al., 2017; Lou & Stucki, 1998; Abedini et al., 2023; Abedini, 2023).

We load the Stanford Bunny mesh using PyVista and construct an undirected graph over its vertices via a k -nearest-neighbors rule, similar to the procedure used in GSPBox. The resulting graph Laplacian defines the graph structure. As a test signal, we consider a non-bandlimited graph signal $\mathbf{f} \in [0, 1]^N$ given by the z -coordinate of each vertex, where N is the number of vertices. We then compute 1-bit halftoned signals $\mathbf{q} \in \{-1, 1\}^N$ using MSQ, SDW, and the proposed SSNS method, and directly visualize \mathbf{q} on the mesh. For both SDW and SSNS, we conduct experiments with two heuristic bandwidth rates, namely $r = 20$ and $r = 50$, see Fig. 6

This experimental design follows the classical motivation of digital halftoning: although the displayed signal is binary,

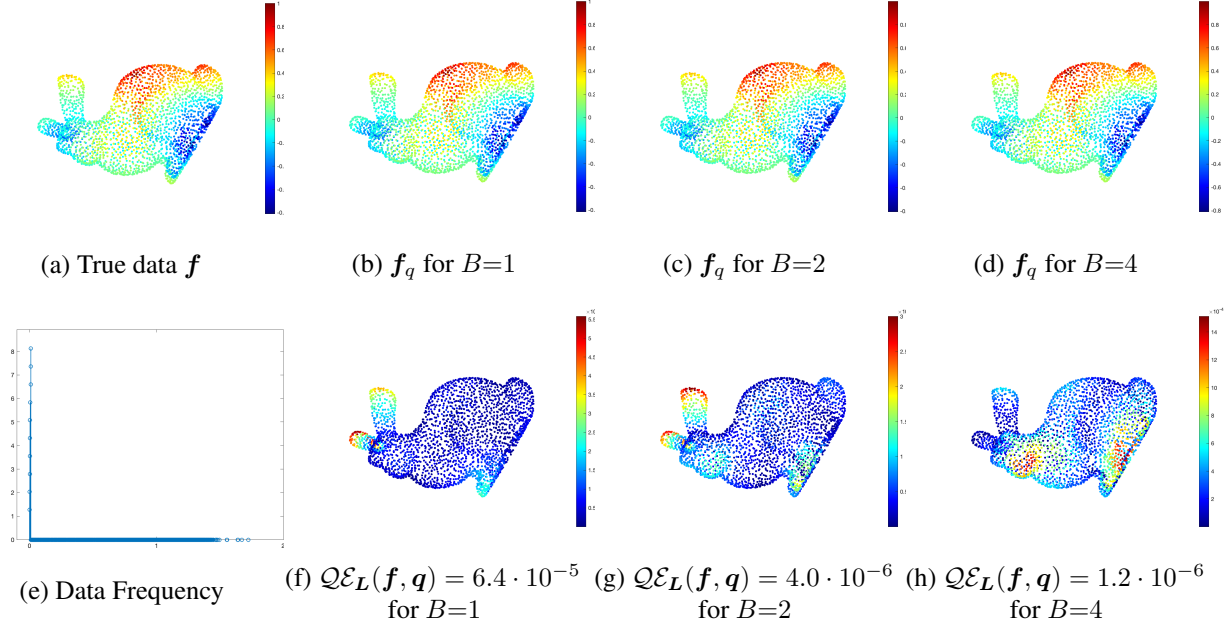


Figure 3. Comparison of the Bunny data and this quantized version: (a) original, (b–d) quantized versions, (e) data frequency spectrum, and (f–h) quantization errors. Each column corresponds to a specific method.

perceptual integration by the human visual system acts as an implicit low-pass filter, so visual appearance is primarily determined by low-frequency content (Floyd & Steinberg, 1976; Lyu & Wang, 2023; Krahmer & Veselovska, 2022). While the signal is not bandlimited and therefore lies outside the scope of our theoretical analysis, the three methods produce visually distinct halftoning patterns, illustrating different ways of shaping quantization artifacts on graphs. We emphasize that with higher bandwidth r , among the compared approaches, only SSNS is supported by provable error bounds, highlighting its role as a theoretically justified alternative for graph-based halftoning.

Experiments — Synopsis. The experiments confirm the effectiveness of our method for quantizing graph data with low bandwidth. The reduction in relative error with increasing bit budget is consistent across all tested graphs, demonstrating the method’s robustness to both signal structure and graph topology.

Furthermore, our results provide insights into the performance scaling of SSNS. Namely, graphs with more uniform connectivity (e.g., 2D grid) tend to exhibit smoother error growth compared to irregular graphs (e.g., sensor or bunny), reflecting the influence of graph topology on the distribution of Fourier energy.

5. Discussion

We have shown in this paper that Single Shot Noise Shaping (SSNS) via Algorithm 1 provides a simple and effective ap-

proach to quantizing graph signals with low computational complexity and predictable scaling behavior. While it is computationally more expensive than existing noise shaping methods such as Step-by-Step-Serving with Replacement (SSS-R), it comes with improved theoretical guarantees, allows for a flexible choice of bit-levels including extreme one-bit quantization, and shows better performance for very small bandwidths.

Limitations. In our study, we focused on the brick-wall filter as a prototype of low-pass filters. Various other low-pass filters exist, such as (Defferrard et al., 2016; Chang et al., 2021; Nt & Maehara, 2019). We furthermore provided no robustness analysis of our method on approximately r -bandlimited data, and only use the graph incoherence to characterize the influence of the graph topology. As our experiment in Figure 3 (f)–(h) suggests, a more refined analysis might be needed to fully explain the observed quantization error on complex graphs for strongly bandlimited signals, cf. Experiment 1 in Section 4.

Impact Statement

This paper aims to advance the field of machine learning, in particular by improving the theoretical understanding of one-bit quantization of graph-structured data as a tool for representing and processing structured graph signals. While there are many potential societal consequences of our work, we do not foresee specific impacts that require separate discussion here.

References

Abedini, F. *2D and 3D Halftoning for Appearance Reproduction*. Linkopings Universitet (Sweden), 2023.

Abedini, F., Hlayhel, R., Gooran, S., Nyström, D., and Sole, A. S. Multi-layer halftoning for poly-jet 3d printing. In *London Imaging Meeting*, volume 4, pp. 30–34. Society for Imaging Science and Technology, 2023.

Ben Saad, L., Beferull-Lozano, B., and Isufi, E. Quantization analysis and robust design for distributed graph filters. *IEEE Transactions on Signal Processing*, 70:643–658, 2022.

Brooks, S. and Lindenstraus, E. Non-localization of eigenfunctions on large regular graphs. *Israel Journal of Mathematics*, 193(1):1–14, 2013.

Chamon, L. F. and Ribeiro, A. Finite-precision effects on graph filters. In *2017 IEEE Global Conference on Signal and Information Processing (GlobalSIP)*, pp. 603–607. IEEE, 2017.

Chang, H., Rong, Y., Xu, T., Bian, Y., Zhou, S., Wang, X., Huang, J., and Zhu, W. Not all low-pass filters are robust in graph convolutional networks. *Advances in Neural Information Processing Systems*, 34:25058–25071, 2021.

Courbariaux, M., Bengio, Y., and David, J.-P. Binaryconnect: Training deep neural networks with binary weights during propagations. *Advances in neural information processing systems*, 28, 2015.

Defferrard, M., Bresson, X., and Vandergheynst, P. Convolutional neural networks on graphs with fast localized spectral filtering. *Advances in neural information processing systems*, 29, 2016.

Dekel, Y., Lee, J. R., and Linial, N. Eigenvectors of random graphs: Nodal domains. *Random Structures & Algorithms*, 39(1):39–58, 2011.

Di Lorenzo, P., Barbarossa, S., and Banelli, P. Optimal power and bit allocation for graph signal interpolation. In *2018 IEEE International Conference on Acoustics, Speech and Signal Processing (ICASSP)*, pp. 4649–4653. IEEE, 2018.

Dong, X., Thanou, D., Frossard, P., and Vandergheynst, P. Learning laplacian matrix in smooth graph signal representations. *IEEE Transactions on Signal Processing*, 64(23):6160–6173, 2016.

Ehler, M., Gräf, M., Neumayer, S., and Steidl, G. Curve based approximation of measures on manifolds by discrepancy minimization. *Foundations of Computational Mathematics*, 21(6):1595–1642, 2021.

Floyd, R. W. An adaptive algorithm for spatial gray-scale. In *Proc. Soc. Inf. Disp.*, volume 17, pp. 75–77, 1976.

Floyd, R. W. and Steinberg, L. An adaptive algorithm for spatial grey scale. *Proceedings of the Society of Information Display*, 17:75–77, 1976.

Fornasier, M. and Hütter, J.-C. Consistency of probability measure quantization by means of power repulsion–attraction potentials. *Journal of Fourier Analysis and Applications*, 22(3):694–749, 2016.

Gooran, S. and Abedini, F. 3d surface structures and 3d halftoning. In *NIP & Digital Fabrication Conference*, volume 36, pp. 75–80. Society for Imaging Science and Technology, 2020.

Gooran, S. and Abedini, F. Three-dimensional adaptive digital halftoning. *Electronic Imaging*, 35:1–12, 2022.

Huang, L., Needell, D., and Tang, S. Robust recovery of bandlimited graph signals via randomized dynamical sampling. *arXiv preprint arXiv:2109.14079*, 2021.

Kim, Y. H. Quantization-aware sampling set selection for bandlimited graph signals. *EURASIP journal on Advances in Signal Processing*, 2022(1):5, 2022.

Kim, Y. H. and Ortega, A. Toward optimal rate allocation to sampling sets for bandlimited graph signals. *IEEE Signal Processing Letters*, 26(9):1364–1368, 2019. doi: 10.1109/LSP.2019.2931397.

Krahmer, F. and Veselovska, A. Enhanced digital halftoning via weighted sigma-delta modulation. *arXiv preprint arXiv:2202.04986*, 2022.

Krahmer, F. and Veselovska, A. Enhanced digital halftoning via weighted sigma-delta modulation. *SIAM Journal on Imaging Sciences*, 16(3):1727–1761, 2023.

Krahmer, F. and Veselovska, A. The mathematics of dots and pixels: On the theoretical foundations of image halftoning. *GAMM-Mitteilungen*, 48(1):e70000, 2025.

Krahmer, F., Lyu, H., Saab, R., Veselovska, A., and Wang, R. Quantization of bandlimited graph signals. In *2023 International Conference on Sampling Theory and Applications (SampTA)*, pp. 1–5. IEEE, 2023.

Krahmer, F., Lyu, H., Saab, R., Qian, J., Veselovska, A., and Wang, R. Low-bit quantization of bandlimited graph signals via iterative methods. *arXiv preprint arXiv:2601.18782*, 2026. doi: 10.48550/arXiv.2601.18782. URL <https://arxiv.org/abs/2601.18782>.

Li, P., Shlezinger, N., Zhang, H., Wang, B., and Eldar, Y. C. Graph signal compression via task-based quantization. In *ICASSP 2021-2021 IEEE International Conference on Acoustics, Speech and Signal Processing (ICASSP)*, pp. 5514–5518. IEEE, 2021.

Li, P., Shlezinger, N., Zhang, H., Wang, B., and Eldar, Y. C. Graph signal compression by joint quantization and sampling. *IEEE transactions on signal processing*, 70: 4512–4527, 2022.

Lou, Q. and Stucki, P. Fundamentals of 3d halftoning. In *International Conference on Raster Imaging and Digital Typography*, pp. 224–239. Springer, 1998.

Lyu, H. and Wang, R. Sigma delta quantization for images. *Communications on Pure and Applied Mathematics*, 76 (5):901–945, 2023.

Maly, J. and Saab, R. A simple approach for quantizing neural networks. *Applied and Computational Harmonic Analysis*, 66:138–150, 2023.

Mao, R., Sarkar, U., Ulichney, R., and Allebach, J. P. 3d halftoning. *Electronic Imaging*, 29:147–155, 2017.

Meyer, P. Quantization of neural networks. *Master's thesis, Ludwig-Maximilians-Universität München*, 2024.

Nobre, I. C. M. and Frossard, P. Optimized quantization in distributed graph signal processing. In *ICASSP 2019-2019 IEEE International Conference on Acoustics, Speech and Signal Processing (ICASSP)*, pp. 5376–5380. IEEE, 2019.

Nt, H. and Maehara, T. Revisiting graph neural networks: All we have is low-pass filters. *arXiv preprint arXiv:1905.09550*, 2019.

Ortega, A., Frossard, P., Kovačević, J., Moura, J. M., and Vandergheynst, P. Graph signal processing: Overview, challenges, and applications. *Proceedings of the IEEE*, 106(5):808–828, 2018.

Pesenson, I. Variational splines and paley–wiener spaces on combinatorial graphs. *Constructive Approximation*, 2009.

Reingruber, P. and Matz, G. Efficient quantization and denoising using local graph fourier frames. In *ICASSP 2025 - 2025 IEEE International Conference on Acoustics, Speech and Signal Processing (ICASSP)*, pp. 1–5, 2025.

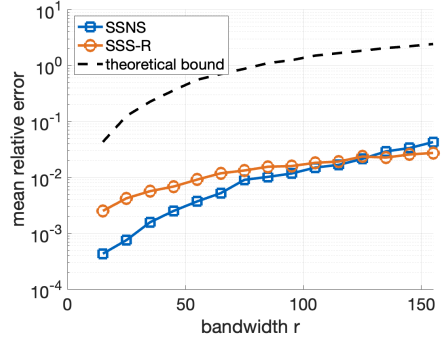
Sandryhaila, A. and Moura, J. M. Big data analysis with signal processing on graphs: Representation and processing of massive data sets with irregular structure. *IEEE signal processing magazine*, 31(5):80–90, 2014.

Shuman, D. I., Narang, S. K., Frossard, P., Ortega, A., and Vandergheynst, P. The emerging field of signal processing on graphs: Extending high-dimensional data analysis to networks and other irregular domains. *IEEE signal processing magazine*, 30(3):83–98, 2013.

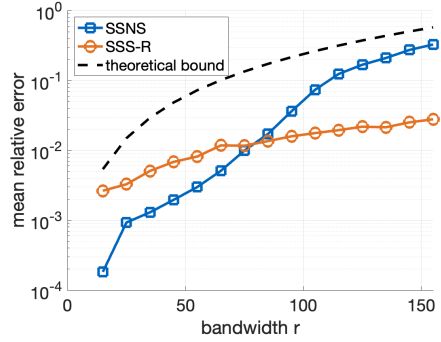
Shuman, D. I., Ricaud, B., and Vandergheynst, P. Vertex-frequency analysis on graphs. *Applied and Computational Harmonic Analysis*, 40(2):260–291, 2016.

Tailor, S. A., Fernandez-Marques, J., and Lane, N. D. Degree-quant: Quantization-aware training for graph neural networks. In *International Conference on Learning Representations*, 2021. URL <https://openreview.net/forum?id=NSBrFgJAHg>.

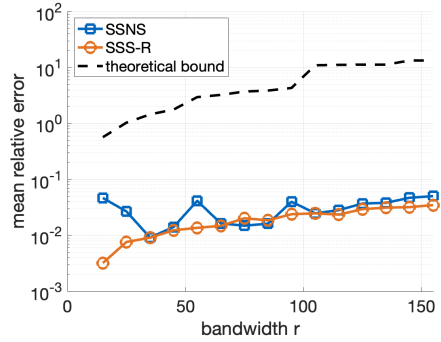
Tanaka, Y. and Eldar, Y. C. Generalized sampling on graphs with subspace and smoothness priors. *IEEE Transactions on Signal Processing*, 68:2272–2286, 2020.



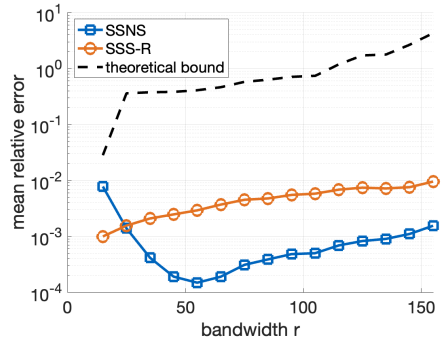
(a) Grid graph



(b) Ring graph



(c) Swiss roll



(d) Bunny graph

Figure 4. Comparison of the performance of SSNS to the theoretical worst-case guarantees 3.1 and to the *Step-by-Step-Serving with Replacement* (SSS-R) method.

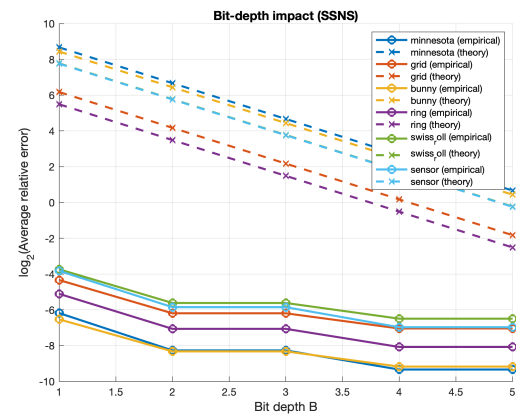


Figure 5. Average relative error versus bit-depth for SSNS across different graph topologies, compared with the theoretical bound proportional to 2^{-B} . Results are averaged over 50 random signals with bandwidth $r = 200$.

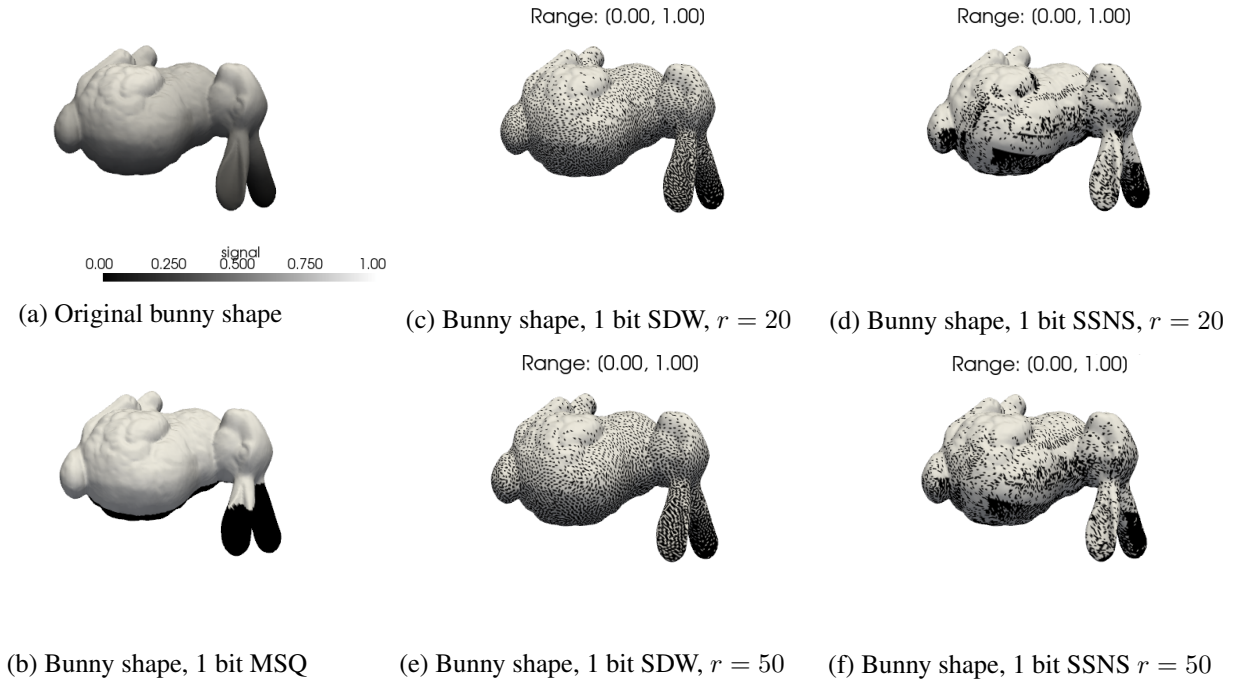


Figure 6. Halftoning of the Stanford Bunny mesh graph signal using 1-bit quantization. (a) Original signal. (b) Memoryless scalar quantization (MSQ). (c),(e) Sigma-Delta-Weight (SDW) (Krahmer et al., 2023) with different bandwidth r . (d),(f) Proposed Single-Shot Noise Shaping (SSNS) with different different bandwidth r . All halftoned outputs are binary signals $q \in \{-1, 1\}^N$ visualized on the mesh.

Algorithm 3 Vector preprocessing (Meyer, 2024)

Input: $\mathbf{X} \in \mathbb{R}^{r \times N}$ ($r < N$), $\mathbf{z}_0 \in \mathbb{R}^N$, and $c \geq \|\mathbf{z}_0\|_\infty$

Initialize $k = 0$ and

$$J_0 = \{i \in [N] : \text{the } i\text{-th column of } \mathbf{X} \text{ is zero}\}.$$

Define $\mathbf{b} \in \mathbb{R}^N$ via $\mathbf{b}_{J_0^c} = \mathbf{0}$ and $b_i = c - (z_0)_i$, for $i \in J_0$, such that $\mathbf{b} \in \ker(\mathbf{X})$ and $|(z_0)_i + b_i| = c$ for $i \in J_0$. Replace \mathbf{z}_0 with $\mathbf{z}_0 + \mathbf{b}$.

repeat

 Let $I = \{i_1, \dots, i_{2r}\} \subset J_k^c$ contain the $2r$ smallest indices in J_k^c .

 Compute a set of r linearly independent vectors $\mathcal{B}^{(1)} = \{\mathbf{b}_1^{(1)}, \dots, \mathbf{b}_r^{(1)}\}$ in $\ker_{I^c}(\mathbf{X})$.

$\mathbf{z}_{k,1} \leftarrow \mathbf{z}_k$

$J_{k,1} \leftarrow J_k$

for $\ell = 1, \dots, r$ **do**

$\mathbf{b} \leftarrow \mathbf{b}_1^{(\ell)}$

 Compute $\alpha \in \mathbb{R}$ with $\|\mathbf{z}_{k,\ell} + \alpha\mathbf{b}\|_\infty = c$

$\mathbf{z}_{k,\ell+1} \leftarrow \mathbf{z}_{k,\ell} + \alpha\mathbf{b} \in \mathbb{R}^N$

$i_* \leftarrow \arg \min\{i \in I : |(\mathbf{z}_{k,\ell+1})_i| = c\}$

$J_{k,\ell+1} \leftarrow J_{k,\ell} \cup \{i_*\}$

 Define $\mathcal{B}^{(\ell+1)} = \{\mathbf{b}_1^{(\ell+1)}, \dots, \mathbf{b}_{r-\ell}^{(\ell+1)}\}$ with

$$\mathbf{b}_j^{(\ell+1)} = \mathbf{b} - \frac{b_{i_*}}{(b_{j+1}^{(\ell)})_{i_*}} \mathbf{b}_{j+1}^{(\ell)},$$

 which consists of $(r - \ell)$ linearly independent vectors with support in $I \setminus J_{k,\ell+1}$.

end for

$J_{k+1} \leftarrow J_{k,r+1}$

$\mathbf{z}_{k+1} \leftarrow \mathbf{z}_{k,r+1}$

$k \leftarrow k + 1$

until $\|\mathbf{z}_k\|_0 - c\mathbf{1} \leq r$

$k_{\text{final}} = k$

Output: $\mathbf{z}_{k_{\text{final}}}$ for which $\mathbf{X}\mathbf{z}_{k_{\text{final}}} = \mathbf{X}\mathbf{z}_0$, $\|\mathbf{z}_{k_{\text{final}}}\|_\infty = c$, and $\|\mathbf{z}_{k_{\text{final}}}\|_0 - c\mathbf{1} \leq r$

Supplementary Material

We provide pseudo-code of the accelerated preprocessing algorithm of Meyer (2024) in Algorithm 3. It improves over Algorithm 1 by extracting kernel vectors \mathbf{b} in a more efficient way. To this end, it splits the columns of \mathbf{X} into blocks of size r and iteratively extracts collections of r kernel vectors per block. By slightly modifying the single kernel vectors in r inner iterations, they can all be used before a new collection has to be generated. Generating r kernel vectors is of the same complexity as generating a single kernel vector. Asymptotically, each of the $\lceil N/r \rceil$ outer iterations of Algorithm 3 thus requires as many operations as each of the N iterations of Algorithm 1, leading to an overall complexity improvement of a factor r .

Note that in our presentation of Algorithm 3 we assume that N is divisible by r for convenience. If this is not the case, the last iteration of the outer loop has to be slightly modified since less than r linearly independent vectors $\mathbf{b}_i^{(1)}$ remain in $\ker_{I^c}(\mathbf{X})$ in the last step.